

# Chiral dynamics of $p$ -wave in $K^-p$ and coupled states

D. Jido<sup>a)1</sup>, E. Oset<sup>b)</sup> and A. Ramos<sup>a)</sup>

<sup>a)</sup> *Departament d'Estructura i Constituents de la Matèria,  
Universitat de Barcelona, Diagonal 647, 08028 Barcelona, Spain*

<sup>b)</sup> *Departamento de Física Teórica and IFIC,  
Centro Mixto Universidad de Valencia-CSIC,  
Ap. Correos 22085, E-46071 Valencia, Spain*

## Abstract

We perform an evaluation of the  $p$ -wave amplitudes of meson-baryon scattering in the strangeness  $S = -1$  sector starting from the lowest order chiral Lagrangians and introducing explicitly the  $\Sigma^*$  field with couplings to the meson-baryon states obtained using SU(6) symmetry. The  $N/D$  method of unitarization is used, equivalent, in practice, to the use of the Bethe-Salpeter equation with a cut-off. The procedure leaves no freedom for the  $p$ -waves once the  $s$ -waves are fixed and thus one obtains genuine predictions for the  $p$ -wave scattering amplitudes, which are in good agreement with experimental results for differential cross sections, as well as for the width and partial decay widths of the  $\Sigma^*(1385)$ .

## 1 Introduction

The advent of chiral perturbation theory ( $\chi PT$ ) as an effective approach to QCD at low energies [1] in hadron dynamics has allowed steady progress in the field of meson-baryon interaction [2, 3, 4, 5]. Yet, an important step in the application of the chiral Lagrangians at higher energies than allowed by  $\chi PT$  is the implementation of unitarity in coupled channels. Pioneering works in this direction were those of [6, 7, 8], where the Lippmann-Schwinger equation in coupled channels was used extracting the kernels from the chiral Lagrangians. Subsequent steps in this direction were done in [9] in the study

---

<sup>1</sup> email address: jido@rcnp.osaka-u.ac.jp, present address: Research Center for Nuclear Physics (RCNP), Ibaraki, Osaka 567-0047, Japan

of the  $K^-p$  interaction with the coupled states using the Bethe-Salpeter equation and introducing all the channels which could be formed from the octet of pseudoscalar mesons and stable baryons. Further steps in this direction in the strangeness  $S = 0$  sector have been done in [10, 11, 12, 13, 14]. The works of [6, 7, 8, 9] deal only about the  $s$ -wave  $K^-p$  scattering, and one obtains a remarkably good agreement at low energies with the data for transitions of  $K^-p$  to different channels, indicating that the  $p$ -wave and higher partial waves play a minor role at these energies. The extension of these works to include  $p$ -wave or higher partial waves is thus desirable in order to see whether the agreement found with only  $s$ -wave is an accident or whether one confirms that the contribution of the  $p$ -wave is indeed small. There is also an important feature of the  $p$ -wave which is the presence of the  $\Sigma(1385)$  resonance appearing with the same quantum numbers as those of the  $K^-p$  system, although only visible in  $\pi\Lambda$  or  $\pi\Sigma$  states since the resonance is below the  $K^-p$  threshold.

The introduction of  $p$ -waves in the strangeness  $S = -1$  sector was done in [15] and more recently in [16, 17]. In [15, 16] only the region of energies above the  $K^-p$  threshold is investigated but the  $\Sigma(1385)$  resonance region is not explored. In [17] the decouplet of the  $\Sigma(1385)$  is explicitly included as a field and new chiral Lagrangians to next to leading order are introduced to deal with the meson-baryon scattering problem. In this latter work the around 25 free parameters of the theory are fitted to the data, although some of the parameters are constrained by large  $N_c$  arguments.

Simplicity is one of the appealing features of the  $K^-p$  interactions from the perspective of chiral symmetry. Indeed, in [9], it was found that using the transition amplitude obtained with the lowest order chiral Lagrangian as a kernel of the Bethe-Salpeter equation, and a cut-off of about 630 MeV to regularize the loops, one could reproduce the cross sections of  $K^-p \rightarrow K^-p$ ,  $\bar{K}^0n$ ,  $\pi^0\Lambda$ ,  $\pi^0\Sigma^0$ ,  $\pi^+\Sigma^-$ ,  $\pi^-\Sigma^+$ , together with the properties of the  $\Lambda(1405)$  resonance, which is dynamically generated in that scheme.

It is remarkable that, using the same input, one can also obtain the  $\Lambda(1670)$  and  $\Sigma(1620)$   $s$ -wave resonances [18] as well as the  $\Xi(1620)$  [19], which completes the octet of lowest energy  $s$ -wave excited baryons together with the  $N^*(1535)$  obtained in [6, 12, 14] following the same lines.

The idea here is to see whether the simplicity observed in the  $s$ -wave interaction holds also for  $p$ -waves. In other words, we would like to see what does one obtain for the  $p$ -wave amplitudes using again the lowest order chiral Lagrangians and the same cut-off parameter as in [9]. Anticipating results, we can say that the  $p$ -wave amplitudes obtained with this line are in good agreement with experiments, as well as the properties of the  $\Sigma(1385)$  resonance, thus obtaining a parameter-free description of the  $p$ -wave phenomenology in the  $S = -1$  sector.

## 2 Meson-baryon amplitudes to lowest order

Following [2, 3, 4, 5] we write the lowest order chiral Lagrangian, coupling the octet of pseudoscalar mesons to the octet of  $1/2^+$  baryons, as

$$\begin{aligned} \mathcal{L}_1^{(B)} = & \langle \bar{B} i \gamma^\mu \nabla_\mu B \rangle - M \langle \bar{B} B \rangle \\ & + \frac{1}{2} D \langle \bar{B} \gamma^\mu \gamma_5 \{u_\mu, B\} \rangle + \frac{1}{2} F \langle \bar{B} \gamma^\mu \gamma_5 [u_\mu, B] \rangle \end{aligned} \quad (1)$$

where the symbol  $\langle \rangle$  denotes the trace of SU(3) flavor matrices,  $M$  is the baryon mass and

$$\begin{aligned} \nabla_\mu B &= \partial_\mu B + [\Gamma_\mu, B], \\ \Gamma_\mu &= \frac{1}{2} (u^\dagger \partial_\mu u + u \partial_\mu u^\dagger), \\ U &= u^2 = \exp(i\sqrt{2}\Phi/f), \\ u_\mu &= iu^\dagger \partial_\mu U u^\dagger. \end{aligned} \quad (2)$$

The couplings  $D$  and  $F$  are chosen as  $D = 0.85$ ,  $F = 0.52$ .

The meson and baryon fields in the SU(3) matrix form are given by

$$\Phi = \begin{pmatrix} \frac{1}{\sqrt{2}}\pi^0 + \frac{1}{\sqrt{6}}\eta & \pi^+ & K^+ \\ \pi^- & -\frac{1}{\sqrt{2}}\pi^0 + \frac{1}{\sqrt{6}}\eta & K^0 \\ K^- & \bar{K}^0 & -\frac{2}{\sqrt{6}}\eta \end{pmatrix}, \quad (3)$$

$$B = \begin{pmatrix} \frac{1}{\sqrt{2}}\Sigma^0 + \frac{1}{\sqrt{6}}\Lambda & \Sigma^+ & p \\ \Sigma^- & -\frac{1}{\sqrt{2}}\Sigma^0 + \frac{1}{\sqrt{6}}\Lambda & n \\ \Xi^- & \Xi^0 & -\frac{2}{\sqrt{6}}\Lambda \end{pmatrix}. \quad (4)$$

The  $BB\Phi\Phi$  interaction Lagrangian comes from the  $\Gamma_\mu$  term in the co-variant derivative and we find

$$\mathcal{L}_1^{(B)} = \left\langle \bar{B} i \gamma^\mu \frac{1}{4f^2} [(\Phi \partial_\mu \Phi - \partial_\mu \Phi \Phi)B - B(\Phi \partial_\mu \Phi - \partial_\mu \Phi \Phi)] \right\rangle, \quad (5)$$

from where one derives the transition amplitudes

$$V_{ij} = -C_{ij} \frac{1}{4f^2} \bar{u}(p') \gamma^\mu u(p) (k_\mu + k'_\mu) \quad (6)$$

where  $k, k'$  ( $p, p'$ ) are the initial and final meson (baryon) momenta, respectively, and the coefficients  $C_{ij}$ , where  $i, j$  indicate the particular meson-baryon channel, form a symmetric matrix and are written explicitly in [9]. Following [9], the meson decay constant  $f$  is taken as an average value  $f = 1.123f_\pi$  [18]. The channels included in our study are  $K^-p, \bar{K}^0n, \pi^0\Lambda,$

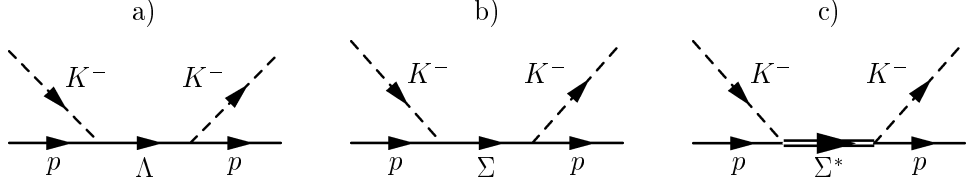


Figure 1: Diagrams for the pole terms of a)  $\Lambda$ , b)  $\Sigma$  and c)  $\Sigma^*$  with the  $K^-p$  channel as an example.

$\pi^0\Sigma^0$ ,  $\eta\Lambda$ ,  $\eta\Sigma^0$ ,  $\pi^+\Sigma^-$ ,  $\pi^-\Sigma^+$ ,  $K^+\Xi^-$ ,  $K^0\Xi^0$ . The  $s$ -wave amplitudes are obtained in [9, 18] and we do not repeat them here. The Lagrangian of eq. (5) provides also a small part of the  $p$ -wave which is easily obtained by evaluating the matrix elements of eq. (6) using the explicit form of the spinor and the Dirac matrices. We obtain, in the center of mass system,

$$t_{ij}^c = -C_{ij} \frac{1}{4f^2} a_i a_j \left( \frac{1}{b_i} + \frac{1}{b_j} \right) (\vec{\sigma} \cdot \vec{k}_j)(\vec{\sigma} \cdot \vec{k}_i) \quad (7)$$

with

$$a_i = \sqrt{\frac{E_i + M_i}{2M_i}}, \quad b_i = E_i + M_i, \quad E_i = \sqrt{M_i^2 + \vec{p}_i^2} \quad (8)$$

where  $M_i$  is the mass of the baryon in channel  $i$ .

In addition we have the contribution from the  $\Lambda$  and  $\Sigma$  pole terms which are obtained from the  $D$  and  $F$  terms of the Lagrangian of eq. (1). The  $\Sigma^*$  pole term is also included explicitly with couplings to the meson-baryon states evaluated using SU(6) symmetry arguments [20]. These terms correspond to the diagrams of Fig. 1 a), b), c).

The amplitudes for the  $\Lambda$ ,  $\Sigma$  and  $\Sigma^*$  pole terms are readily evaluated and performing a nonrelativistic reduction, keeping terms up to  $\mathcal{O}(p/M)$ , we find in the center of mass frame,

$$\begin{aligned} t_{ij}^\Lambda &= D_i^\Lambda D_j^\Lambda \frac{1}{\sqrt{s} - \tilde{M}_\Lambda} (\vec{\sigma} \cdot \vec{k}_j)(\vec{\sigma} \cdot \vec{k}_i) \left( 1 + \frac{k_j^0}{M_j} \right) \left( 1 + \frac{k_i^0}{M_i} \right), \\ t_{ij}^\Sigma &= D_i^\Sigma D_j^\Sigma \frac{1}{\sqrt{s} - \tilde{M}_\Sigma} (\vec{\sigma} \cdot \vec{k}_j)(\vec{\sigma} \cdot \vec{k}_i) \left( 1 + \frac{k_j^0}{M_j} \right) \left( 1 + \frac{k_i^0}{M_i} \right), \\ t_{ij}^{\Sigma^*} &= D_i^{\Sigma^*} D_j^{\Sigma^*} \frac{1}{\sqrt{s} - \tilde{M}_{\Sigma^*}} (\vec{S} \cdot \vec{k}_j)(\vec{S}^\dagger \cdot \vec{k}_i) \end{aligned} \quad (9)$$

with  $S^\dagger$  the spin transition operator from spin 1/2 to 3/2 with the property

$$\sum_{M_s} S_i |M_s\rangle \langle M_s| S_j^\dagger = \frac{2}{3} \delta_{ij} - \frac{i}{3} \epsilon_{ijk} \sigma_k \quad (10)$$

|                    | $K^-p$                 | $\bar{K}^0n$           | $\pi^0\Lambda$       | $\pi^0\Sigma^0$      | $\eta\Lambda$         | $\eta\Sigma^0$        | $\pi^+\Sigma^-$        | $\pi^-\Sigma^+$       | $K^+\Xi^-$             | $K^0\Xi^0$             |
|--------------------|------------------------|------------------------|----------------------|----------------------|-----------------------|-----------------------|------------------------|-----------------------|------------------------|------------------------|
| $c_i^{D,\Lambda}$  | $-\sqrt{\frac{1}{20}}$ | $-\sqrt{\frac{1}{20}}$ | 0                    | $\sqrt{\frac{1}{5}}$ | $-\sqrt{\frac{1}{5}}$ | 0                     | $\sqrt{\frac{1}{5}}$   | $\sqrt{\frac{1}{5}}$  | $-\sqrt{\frac{1}{20}}$ | $-\sqrt{\frac{1}{20}}$ |
| $c_i^{F,\Lambda}$  | $\sqrt{\frac{1}{4}}$   | $\sqrt{\frac{1}{4}}$   | 0                    | 0                    | 0                     | 0                     | 0                      | 0                     | $-\sqrt{\frac{1}{4}}$  | $-\sqrt{\frac{1}{4}}$  |
| $c_i^{D,\Sigma}$   | $\sqrt{\frac{3}{20}}$  | $-\sqrt{\frac{3}{20}}$ | $\sqrt{\frac{1}{5}}$ | 0                    | 0                     | $\sqrt{\frac{1}{5}}$  | 0                      | 0                     | $\sqrt{\frac{3}{20}}$  | $-\sqrt{\frac{3}{20}}$ |
| $c_i^{F,\Sigma}$   | $\sqrt{\frac{1}{12}}$  | $-\sqrt{\frac{1}{12}}$ | 0                    | 0                    | 0                     | 0                     | $-\sqrt{\frac{1}{3}}$  | $\sqrt{\frac{1}{3}}$  | $-\sqrt{\frac{1}{12}}$ | $\sqrt{\frac{1}{12}}$  |
| $c_i^{S,\Sigma^*}$ | $-\sqrt{\frac{1}{12}}$ | $\sqrt{\frac{1}{12}}$  | $\sqrt{\frac{1}{4}}$ | 0                    | 0                     | $-\sqrt{\frac{1}{4}}$ | $-\sqrt{\frac{1}{12}}$ | $\sqrt{\frac{1}{12}}$ | $\sqrt{\frac{1}{12}}$  | $-\sqrt{\frac{1}{12}}$ |

Table 1:  $c^D$ ,  $c^F$ ,  $c^S$  coefficients of eq. (9).

and

$$\begin{aligned}
D_i^\Lambda &= c_i^{D,\Lambda} \sqrt{\frac{20}{3}} \frac{D}{2f} - c_i^{F,\Lambda} \sqrt{12} \frac{F}{2f}, \\
D_i^\Sigma &= c_i^{D,\Sigma} \sqrt{\frac{20}{3}} \frac{D}{2f} - c_i^{F,\Sigma} \sqrt{12} \frac{F}{2f}, \\
D_i^{\Sigma^*} &= c_i^{S,\Sigma^*} \frac{12}{5} \frac{D+F}{2f}.
\end{aligned} \tag{11}$$

The constants  $c^D$ ,  $c^F$ ,  $c^S$  are SU(3) Clebsch-Gordan coefficients which depend upon the meson and baryon involved in the vertex and are given in Table 1. The phase relating physical states to isospin states  $|K^-\rangle = -|1/2, 1/2\rangle$ ,  $|\Xi^-\rangle = -|1/2, 1/2\rangle$ ,  $|\pi^+\rangle = -|1, 1\rangle$ ,  $|\Sigma^+\rangle = -|1, 1\rangle$ , normally adopted in the chiral Lagrangians, are also assumed here.  $\tilde{M}_\Lambda$ ,  $\tilde{M}_\Sigma$ ,  $\tilde{M}_{\Sigma^*}$  are bare masses of the hyperons, which will turn into physical masses upon unitarization.

### 3 Unitary amplitudes

The lowest order (tree level) contributions to the  $p$ -wave meson-baryon scattering matrix are provided by eqs. (7) and (9). Following the philosophy of [9], the tree level contributions are used as a kernel of the Bethe-Salpeter equation. Furthermore, the factorization of the kernel makes it technically simpler to solve the Bethe-Salpeter equation. It was shown in [9] that the kernel for the  $s$ -wave amplitudes can be factorized on the mass shell in the loop functions, by making some approximations typical of heavy baryon perturbation theory. The factorization for  $p$ -waves in meson-meson scattering is also proved in [21] along the same lines. A different, more general, proof of the factorization is done in [22] for meson-meson interactions and in [16] for meson-baryon ones where, using the  $N/D$  method of unitarization and performing dispersion relations, one proves the on-shell factorization in the absence of the left-hand cut contribution. This part is shown to be small

in [22] for meson-meson scattering and even smaller for the meson-baryon case because of the large baryonic masses in the meson-baryon systems. The formal result obtained in [16] for the meson-baryon amplitudes in the different channels is given in matrix form by the same result coming from the Bethe-Salpeter equation

$$T = V + VGT , \quad (12)$$

that is

$$T = [1 - VG]^{-1}V \quad (13)$$

where  $V$  is the kernel (potential), given by the amplitudes of eqs. (7) and (9), and  $G$  is a diagonal matrix accounting for the loop function of a meson-baryon propagator, which must be regularized to eliminate the infinities. In [9] it was regularized by means of a cut-off, while in [16] dimensional regularization was used. Both methods are eventually equivalent although in the dimensional regularization scheme there is a different subtraction constant in each isospin channel and thus allows for more freedom.

The loop function  $G$  in the cut-off method is given by

$$\begin{aligned} G_l(\sqrt{s}) &= i \int \frac{d^4q}{(2\pi)^4} \frac{M_l}{E_l(\vec{q})} \frac{1}{k^0 + p^0 - q^0 - E_l(\vec{q}) + i\epsilon} \frac{1}{q^2 - m_l^2 + i\epsilon} \quad (14) \\ &= \int^{q_{\max}} \frac{d^3q}{(2\pi)^3} \frac{1}{2\omega_l(q)} \frac{M_l}{E_l(q)} \frac{1}{p^0 + k^0 - \omega_l(q) - E_l(q)} \end{aligned}$$

while in dimensional regularization one has

$$\begin{aligned} G_l(\sqrt{s}) &= i2M_l \int \frac{d^4q}{(2\pi)^4} \frac{1}{(P-q)^2 - M_l^2 + i\epsilon} \frac{1}{q^2 - m_l^2 + i\epsilon} \\ &= \frac{2M_l}{16\pi^2} \left\{ a(\mu) + \ln \frac{M_l^2}{\mu^2} + \frac{m_l^2 - M_l^2 + s}{2s} \ln \frac{m_l^2}{M_l^2} \right. \quad (15) \\ &\quad + \frac{\bar{q}_l}{\sqrt{s}} \left[ \ln(s - (M_l^2 - m_l^2) + 2\bar{q}_l\sqrt{s}) + \ln(s + (M_l^2 - m_l^2) + 2\bar{q}_l\sqrt{s}) \right. \\ &\quad \left. \left. - \ln(-s + (M_l^2 - m_l^2) + 2\bar{q}_l\sqrt{s}) - \ln(-s - (M_l^2 - m_l^2) + 2\bar{q}_l\sqrt{s}) \right] \right\} , \end{aligned}$$

where  $m$  and  $M$  are taken to be the observed meson and baryon masses, respectively, in order to respect the phase space allowed by the physical states, and  $\mu$  is a regularization scale (playing the role of a cut-off) and  $a_i$  are subtraction constants in each of the isospin channels. In [18] it was shown that, taking  $\mu = 630$  MeV as the cut-off in [9], the values of the subtraction constants in eq. (15) which lead to the same results as in the cut-off scheme are <sup>2</sup>

$$a_{\bar{K}N} = -1.84, \quad a_{\pi\Sigma} = -2.00, \quad a_{\pi\Lambda} = -1.83$$

---

<sup>2</sup>The  $a_{K\Xi}$  parameter quoted here is slightly changed from  $-2.56$  in [18] in order to get the position of the  $\Lambda(1670)$  resonance better, but as show there, this parameters has no relevance in the low energy results studied here.

$$a_{\eta\Lambda} = -2.25, \quad a_{\eta\Sigma} = -2.38, \quad a_{K\Xi} = -2.67. \quad (16)$$

We shall use the same values here and hence this procedure would be equivalent to performing the calculations using a unique cut-off  $q_{\max} = 630$  MeV in all channels. In a second step we shall relax this constraint and allow the subtraction constants to vary freely to obtain a better global fit to the data.

The use of the amplitudes of eqs. (7) and (9) directly in eq. (13) is impractical since, due to their spin structure, there is a mixture of different angular momenta. It is standard to separate the amplitude for a spin zero meson and a spin 1/2 baryon into different angular momentum components. We write, with the angle  $\theta$  between meson momenta in initial and final states,

$$f(\vec{k}', \vec{k}) = \sum_{l=0}^{\infty} \{(l+1)f_{l+} + lf_{l-}\} P_l(\cos\theta) - i\vec{\sigma} \cdot (\hat{k}' \times \hat{k}) \sum_{l=0}^{\infty} \{f_{l+} - f_{l-}\} P_l'(\cos\theta), \quad (17)$$

which separates the amplitude into a spin non-flip part and a spin flip one. The amplitudes  $f_{l+}$ ,  $f_{l-}$  correspond to orbital angular momentum  $l$  and total angular momentum  $l+1/2$ ,  $l-1/2$ , respectively. These amplitudes exhibit independent unitarity conditions and separate in the Bethe-Salpeter equation. If we specify the  $l=1$  case, the  $p$ -wave amplitudes can be written as

$$T(\vec{k}', \vec{k}) = (2l+1) \left( f(\sqrt{s}) \hat{k}' \cdot \hat{k} - ig(\sqrt{s}) (\hat{k}' \times \hat{k}) \cdot \vec{\sigma} \right) \quad (l=1). \quad (18)$$

From Eqs. (7), (9) the corresponding lowest order (tree level) amplitudes read

$$f_{ij}^{\text{tree}}(\sqrt{s}) = \frac{1}{3} \left\{ -C_{ij} \frac{1}{4f^2} a_i a_j \left( \frac{1}{b_i} + \frac{1}{b_j} \right) + \frac{D_i^\Lambda D_j^\Lambda \left( 1 + \frac{k_i^0}{M_i} \right) \left( 1 + \frac{k_j^0}{M_j} \right)}{\sqrt{s} - \tilde{M}_\Lambda} + \frac{D_i^\Sigma D_j^\Sigma \left( 1 + \frac{k_i^0}{M_i} \right) \left( 1 + \frac{k_j^0}{M_j} \right)}{\sqrt{s} - \tilde{M}_\Sigma} + \frac{2}{3} \frac{D_i^{\Sigma*} D_j^{\Sigma*}}{\sqrt{s} - \tilde{M}_\Sigma^*} \right\} k_i k_j \quad (19)$$

$$g_{ij}^{\text{tree}}(\sqrt{s}) = \frac{1}{3} \left\{ C_{ij} \frac{1}{4f^2} a_i a_j \left( \frac{1}{b_i} + \frac{1}{b_j} \right) - \frac{D_i^\Lambda D_j^\Lambda \left( 1 + \frac{k_i^0}{M_i} \right) \left( 1 + \frac{k_j^0}{M_j} \right)}{\sqrt{s} - \tilde{M}_\Lambda} - \frac{D_i^\Sigma D_j^\Sigma \left( 1 + \frac{k_i^0}{M_i} \right) \left( 1 + \frac{k_j^0}{M_j} \right)}{\sqrt{s} - \tilde{M}_\Sigma} + \frac{1}{3} \frac{D_i^{\Sigma*} D_j^{\Sigma*}}{\sqrt{s} - \tilde{M}_\Sigma^*} \right\} k_i k_j \quad (20)$$

where  $i, j$  are channel indices. Hence, denoting  $f_{l+} \equiv f_+$ ,  $f_{l-} \equiv f_-$  for  $l=1$ , with

$$f_+ = f + g \quad (21)$$

$$f_- = f - 2g ,$$

and using Eq. (13), one obtains

$$\begin{aligned} f_+ &= [1 - f_+^{\text{tree}} G]^{-1} f_+^{\text{tree}} \\ f_- &= [1 - f_-^{\text{tree}} G]^{-1} f_-^{\text{tree}} . \end{aligned} \quad (22)$$

As one can see from these equations, the amplitudes  $f_+^{\text{tree}}$ ,  $f_-^{\text{tree}}$  in the diagonal meson-baryon channels contain the factor  $\vec{k}^2$ , with  $\vec{k}$  the on-shell center-of-mass momentum of the meson in this channel. For transition matrix elements from channel  $i$  to  $j$  the corresponding factor is  $k_i k_j$  where the energy and momentum of the meson in a certain channel are given by

$$E_i = \frac{s + m_i^2 - M_i^2}{2\sqrt{s}} ; \quad k_i = \sqrt{E_i^2 - m_i^2} , \quad (23)$$

which also provides the analytical extrapolation below the threshold of the channel where  $k_i$  becomes purely imaginary.

The differential cross sections, including the  $s$ -wave amplitudes are given by

$$\frac{d\sigma_{ij}}{d\Omega} = \frac{1}{16\pi^2} \frac{M_i M_j}{s} \frac{k'}{k} \left\{ |f^{(s)} + (2f_+ + f_-) \cos \theta|^2 + |f_+ - f_-|^2 \sin^2 \theta \right\} \quad (24)$$

where the subscript  $i, j$  in each of the amplitudes must be understood. The set of equations (22) can be solved in the space of physical states, the ten-channel space introduced in the former section. Alternatively one can also construct states of given isospin (see section 3 of Ref. [9]) and work directly with isospin states. Conversely, one can work with the physical states and construct the isospin amplitudes from the appropriate linear combinations of transition amplitudes with physical states. The isospin separation is useful for  $p$ -wave. Indeed in the channel  $f_-$ , which corresponds to  $J = 1/2$ , we can have  $I = 0, I = 1$ . The pole of the  $\Lambda$  and the  $\Sigma$  from the pole terms in Fig. 1 will show up in the calculation in these channels, respectively. However, the unitarization procedure will shift the mass from a starting bare mass  $\tilde{M}_\Lambda, \tilde{M}_\Sigma$  in eqs. (9) to another mass which we demand to be the physically observed mass. Similarly, in the  $f_+$  amplitude, corresponding to  $J = 3/2$ , there will be a pole for  $I = 1$  corresponding to the  $\Sigma^*$ . Once again we start from a bare mass  $\tilde{M}_{\Sigma^*}$  in eqs. (9) such that after unitarization the pole appears at the physical  $\Sigma^*$  mass. In the case of the  $\Sigma^*$ , since there is phase space for decay into  $\pi\Sigma$  and  $\pi\Lambda$ , the unitarization procedure will automatically provide the width of the  $\Sigma^*$ . With no free parameters to play with, the results obtained for the  $\Sigma^*$  width and the branching ratios to the  $\pi\Sigma$  and  $\pi\Lambda$  channels will be genuine predictions of the theoretical framework. Since the poles of the coupled channel  $T$  matrix appear when the determinant of the  $[1 - f_+^{\text{tree}} G]$  or  $[1 - f_-^{\text{tree}} G]$  matrices is zero (in the complex plane), it is clear from Eq. (22) that one gets the same  $\Lambda, \Sigma$  or  $\Sigma^*$  poles in all the matrix elements.



## 4 Results

In Fig. 2, we can see the total cross sections for  $K^-p$  to different channels as a function of the initial meson momentum in the laboratory frame. The parameters taken there are the set of values of the subtraction constants  $a_i$  from eq. (16) which are already fixed from [18], and the values of the bare masses,  $\tilde{M}_\Lambda = 1078$  MeV,  $\tilde{M}_\Sigma = 1104$  MeV,  $\tilde{M}_{\Sigma^*} = 1359$  MeV. The results with the  $s$ -wave alone are equivalent to those presented in [9]. As already remarked there, the agreement with experiment is quite good, particularly taking into account that only a free parameter, the cut-off, has been fitted to the data. In addition the threshold ratios  $\gamma$ ,  $R_c$ ,  $R_n$  defined as

$$\begin{aligned}\gamma &= \frac{\Gamma(K^-p \rightarrow \pi^+\Sigma^-)}{\Gamma(K^-p \rightarrow \pi^-\Sigma^+)} = 2.36 \pm 0.04 \\ R_c &= \frac{\Gamma(K^-p \rightarrow \text{charged particles})}{\Gamma(K^-p \rightarrow \text{all})} = 0.664 \pm 0.011 \\ R_n &= \frac{\Gamma(K^-p \rightarrow \pi^0\Lambda)}{\Gamma(K^-p \rightarrow \text{all neutral states})} = 0.189 \pm 0.015\end{aligned}\quad (25)$$

were also well reproduced. The values obtained here are  $\gamma = 2.30$ ,  $R_c = 0.618$ ,  $R_n = 0.257$ .

The effect of adding the  $p$ -wave is quite small in the cross sections, justifying the success of the results obtained using the  $s$ -wave alone. In order to better appreciate the effect of the  $p$ -wave, it is better to look at the differential cross sections since there one is sensitive to the interference of  $s$ - and  $p$ -waves, which results in larger effects than in the integrated cross section where just the square of the  $p$ -wave amplitudes appears. We can see in Fig. 3 that the incorporation of the  $p$ -waves provides the right slope in the differential cross sections, clearly indicating that the amount of  $p$ -wave introduced is the correct one. The agreement is not perfect for all laboratory momenta shown, but the little strength missing or in excess is clearly due to the dominant  $s$ -wave. In order to emphasize this better we have taken advantage of the fact that one can make a fine-tuning of the subtraction constants  $a_i$  to improve the fit to the data. We have just changed the parameters  $a_i$  slightly to the values

$$\begin{aligned}a_{\bar{K}N} &= -1.75, & a_{\pi\Sigma} &= -2.10, & a_{\pi\Lambda} &= -1.62 \\ a_{\eta\Lambda} &= -2.56, & a_{\eta\Sigma} &= -1.54, & a_{K\Xi} &= -2.67\end{aligned}\quad (26)$$

by means of which one obtains improved values for the low energy observables:

$$\gamma = 2.36, \quad R_c = 0.634, \quad R_n = 0.178. \quad (27)$$

The values of the bare masses are now  $\tilde{M}_\Lambda = 1069$  MeV,  $\tilde{M}_\Sigma = 1195$  MeV,  $\tilde{M}_{\Sigma^*} = 1413$  MeV. The results for the integrated cross sections with this new

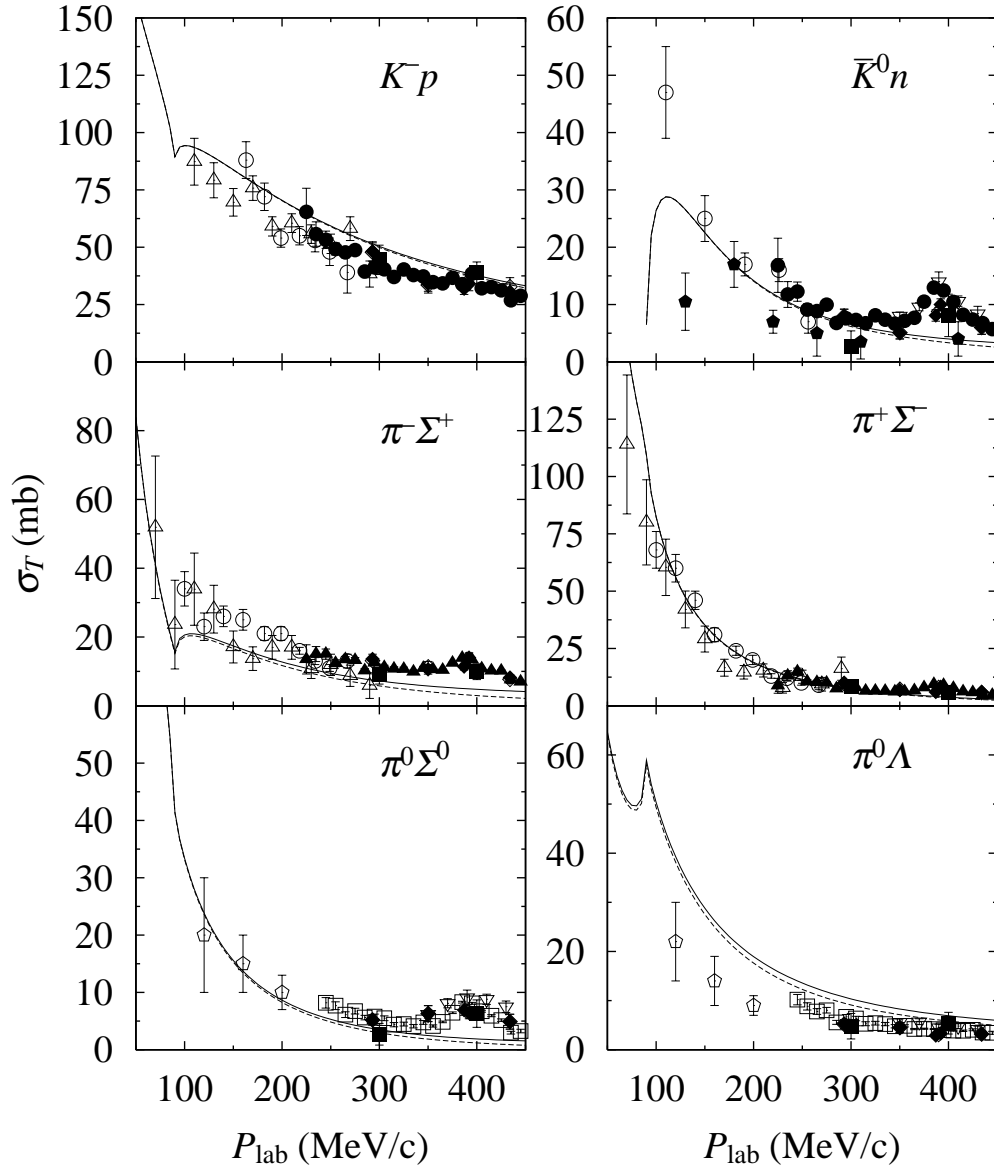


Figure 2: Total cross sections of the  $K^-p$  elastic and inelastic scatterings. The solid line denotes our results with the parameter set of Eq. (16) including both  $s$ -wave and  $p$ -wave. The dashed line shows our results without the  $p$ -wave amplitudes. The data are taken from : [23] (open circles), [24] (black triangles), [25] (black circles), [26] (open triangles), [27] (open squares), [28] (black squares), [29] (open down triangles), [30] (open diamonds), [31] (black diamonds), [32] (open pentagons) and [33] (black pentagons).

set of parameters are shown in Fig. 4. The improvement is clearly appreciable in the  $K^-p \rightarrow K^-p$  and  $K^-p \rightarrow \pi^0\Lambda$  cross sections. The effect of the  $p$ -waves are more clearly shown in Fig. 5, where the differential cross sections for  $K^-p \rightarrow K^-p$  and  $K^-p \rightarrow \bar{K}^0n$  are now well reproduced. In fact, the  $p$ -waves have barely changed from Fig. 3 to Fig. 5, but the slight improvement in the  $s$ -wave brings the results in better agreement with experiment. It is interesting to mention that there has been no free parameter in the determination of the  $p$ -wave amplitude. The bare masses of the  $\Lambda$ ,  $\Sigma$ ,  $\Sigma^*$  cannot be considered free parameters since they are determined by the physical masses of the baryons once the regularizing cut-off is chosen.

## 5 Properties of the $\Sigma^*(1385)$ resonance

We turn now to the results below threshold where the  $\Sigma^*(1385)$  resonance appears. The results are seen in the  $\pi\Lambda$  or  $\pi\Sigma$  mass distributions in reactions with  $\pi\Lambda$  or  $\pi\Sigma$  in the final state. The mass distribution of  $\pi\Lambda$  is given by

$$\frac{d\sigma}{dm} = C \left| t_{\pi\Lambda \rightarrow \pi\Lambda}^{(I=1)} \right|^2 p_{\text{CM}}(\Lambda) , \quad (28)$$

where the constant  $C$  is related to the particular reaction generating the  $\pi\Lambda$  state prior to final state interactions. Relatedly, the  $\pi\Sigma$  mass distribution originating from the same primary mechanism will be given by Eq. 28 by changing  $\left| t_{\pi\Lambda \rightarrow \pi\Lambda}^{(I=1)} \right|^2 p_{\text{CM}}(\Lambda)$  by  $\left| t_{\pi\Lambda \rightarrow \pi\Sigma}^{(I=1)} \right|^2 p_{\text{CM}}(\Sigma)$ . The shape of the mass distribution is used experimentally to obtain the position and width of the resonance, and the ratio of partial widths of  $\Sigma^* \rightarrow \pi\Lambda, \pi\Sigma$  can be obtained by means of

$$\frac{\Gamma_{\pi\Lambda}}{\Gamma_{\pi\Sigma}} = \frac{\left| t_{\pi\Lambda \rightarrow \pi\Lambda}^{(I=1)} \right|^2 p_{\text{CM}}(\Lambda)}{\left| t_{\pi\Lambda \rightarrow \pi\Sigma}^{(I=1)} \right|^2 p_{\text{CM}}(\Sigma)} . \quad (29)$$

In Fig. 6 we can see the shape of the  $\Sigma^*$  distribution, which a width of about  $\Gamma_{\Sigma^*} \simeq 31$  MeV which compares favorably with the experimental value of  $\Gamma_{\Sigma^*} \simeq 35 \pm 4$  MeV [35]. The ratio of the partial decay widths obtained is

$$\frac{\Gamma_{\pi\Lambda}}{\Gamma_{\pi\Sigma}} = 7.7 , \quad (30)$$

which compares well with the experimental value of  $7.5 \pm 0.5$ .

We have looked for poles in the complex plane in the  $p$ -wave amplitudes and have not found any, except for the  $\Sigma^*(1385)$  which is introduced as a genuine resonance in our approach, in the same way as the  $\Lambda$  or  $\Sigma$  baryons are included as basic fields in the theory. This means that the strength of the lowest order  $p$ -wave amplitudes is too weak to generate dynamical resonances, contrary to what was found in [18] for the  $s$ -waves.

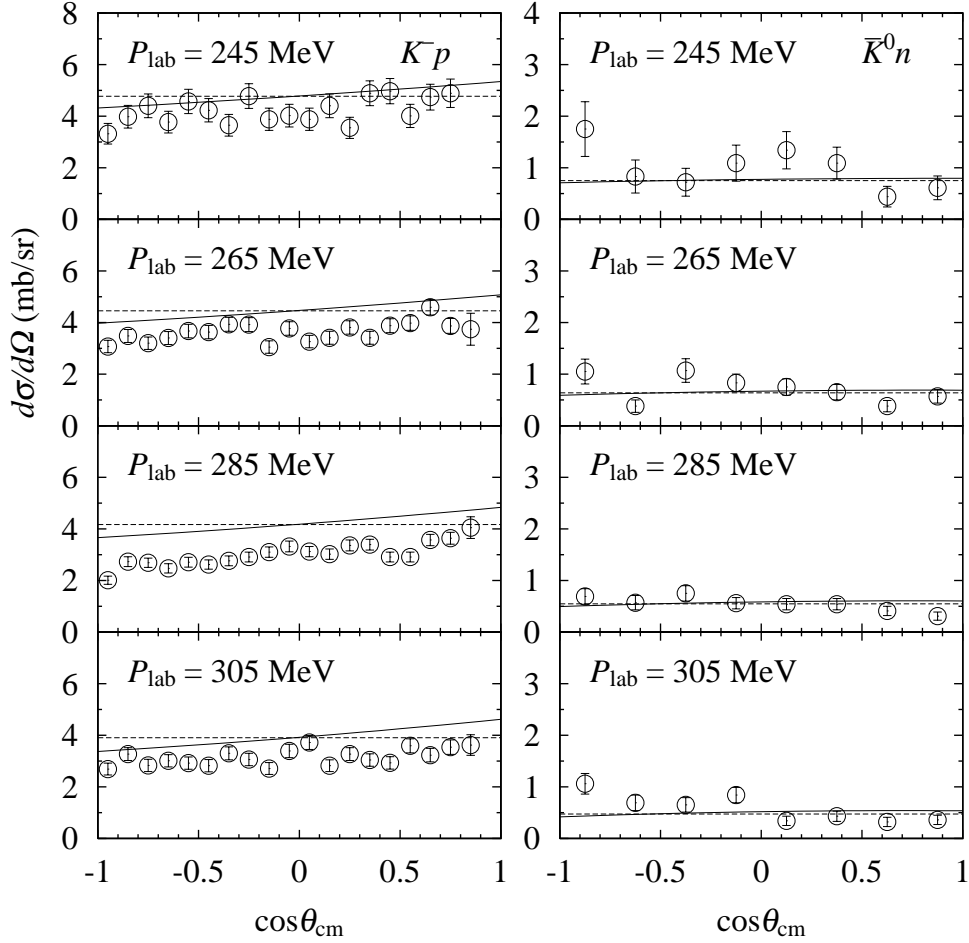


Figure 3: Differential cross sections of the  $K^-p \rightarrow K^-p$ ,  $\bar{K}^0n$  scatterings at  $p_{\text{lab}} = 245, 265, 285$  and  $305$  MeV. The solid line denotes our results with the parameter set of Eq. (16) including both  $s$ -wave and  $p$ -wave. The dashed line shows our results without the  $p$ -wave amplitudes. The data are taken from [25].

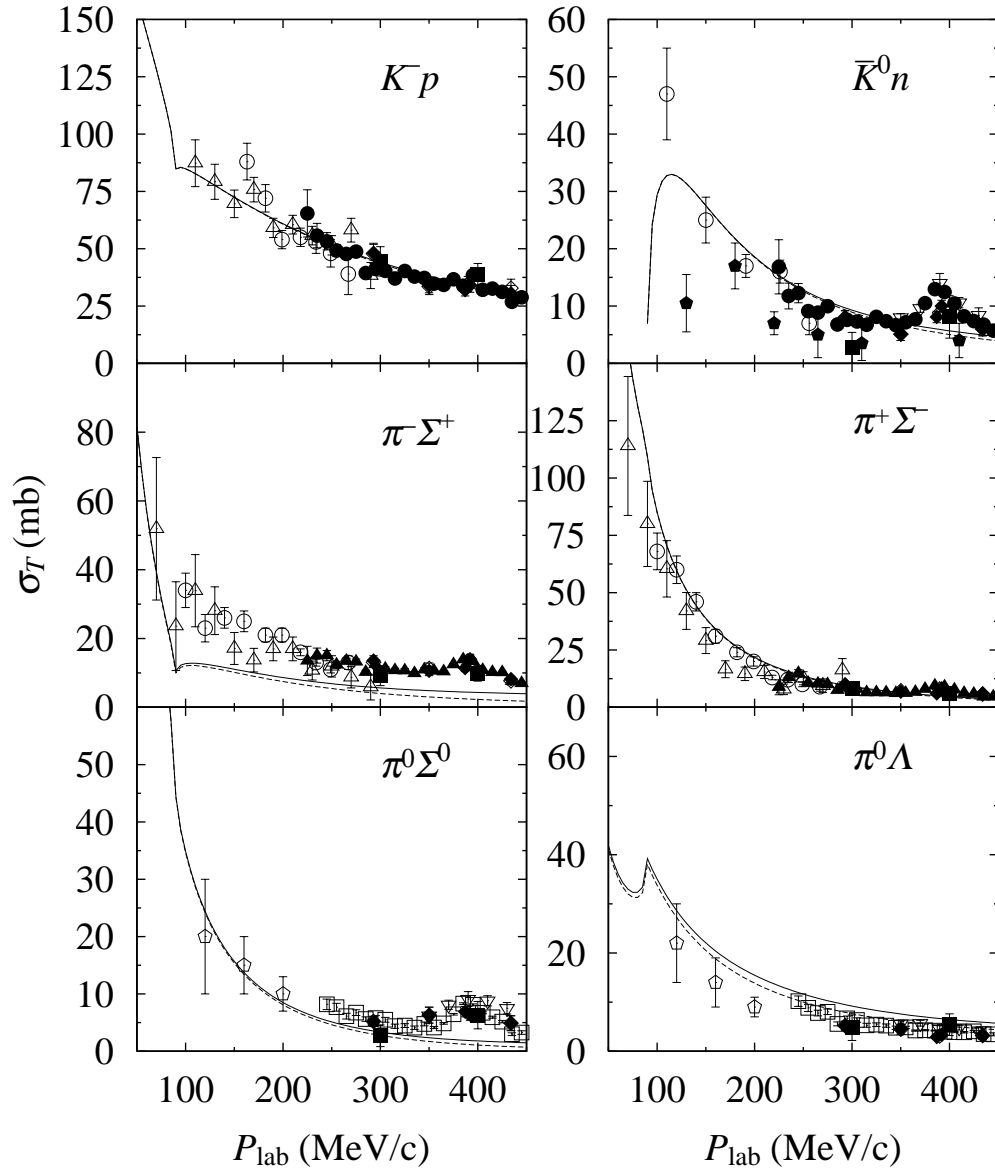


Figure 4: Same as Fig. 2 with the parameter set of Eq. (26).

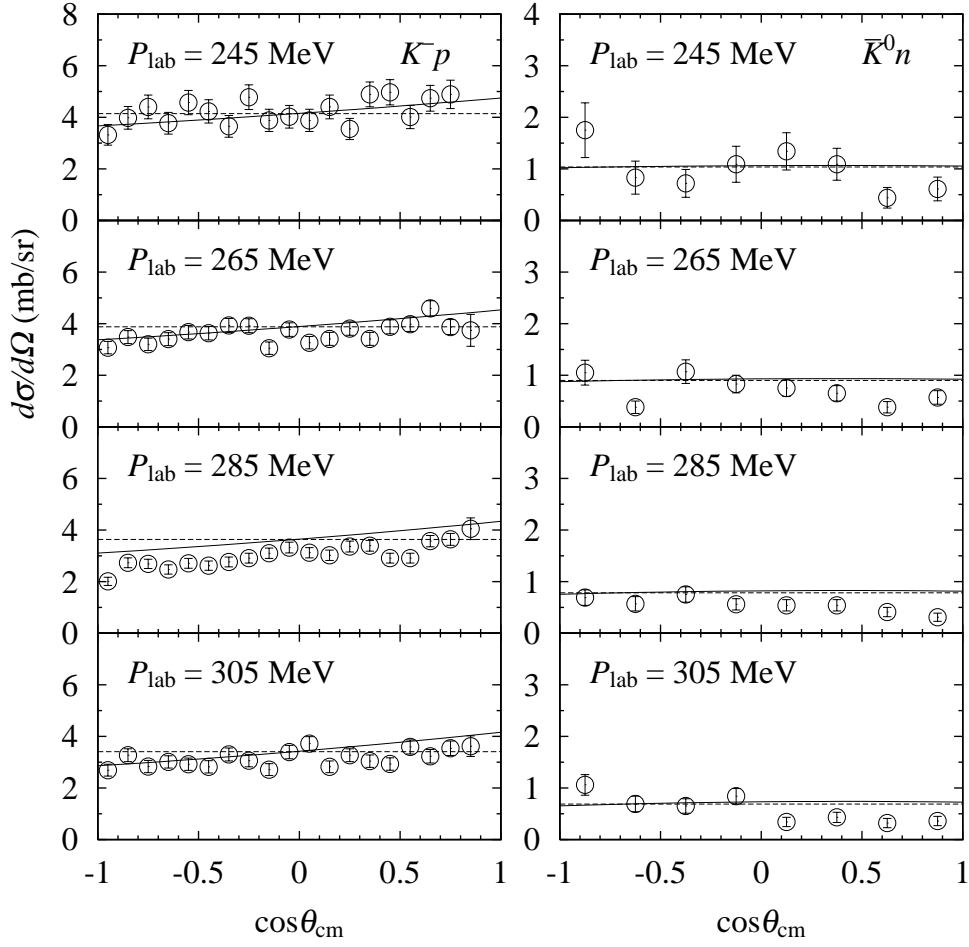


Figure 5: Same as Fig. 3 with the parameter set of Eq. (26).

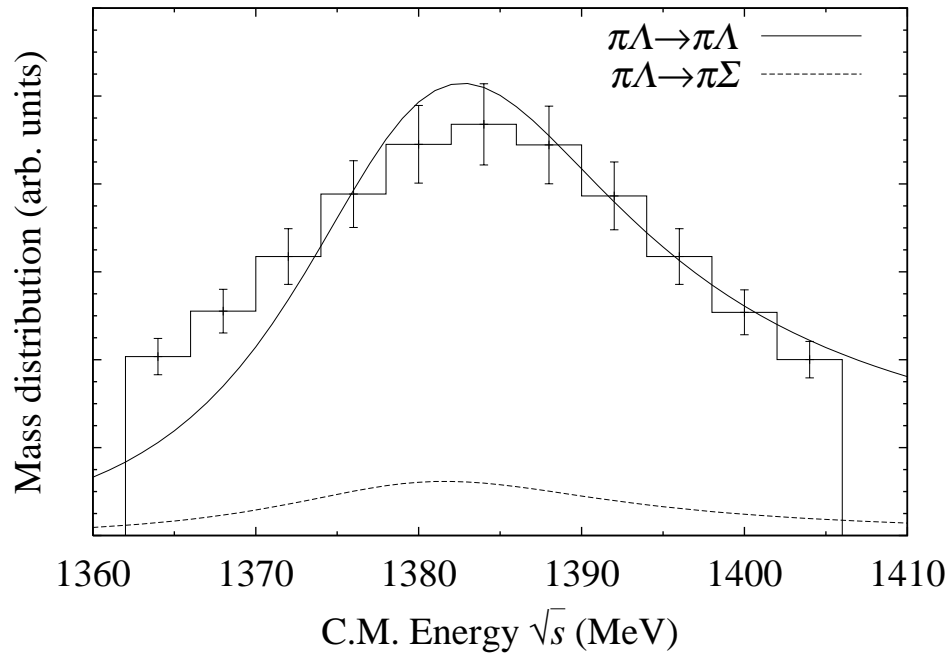


Figure 6:  $\Sigma^*(1385)$  mass distributions in arbitrary units. The solid lines denotes the mass distribution in the  $\pi\Lambda \rightarrow \pi\Lambda$  reaction, while the dashed line shows the one for the  $\pi\Sigma$  with  $I = 1$  in the final state. The data are taken from [34].

## 6 Conclusions

We have evaluated the  $p$ -wave amplitudes for meson-baryon scattering in the strangeness  $S = -1$  sector starting from the lowest order chiral Lagrangian, unitarizing by means of the Bethe-Salpeter equation, or equivalently the  $N/D$  method, and regularizing the loops with a cut-off or an equivalent method using dimensional regularization. The cut-off, or equivalently the subtraction constants in the dimensional regularization procedure, is fitted to the scattering observables at threshold. In practice we take them from earlier work [18] where only the  $s$ -wave amplitudes were studied in our approach. Once this is done there is no extra freedom for the  $p$ -wave amplitudes, which are completely determined in our approach. We perform some fine-tuning of the subtraction constants with respect to [18] in order to obtain better results for the  $K^-p \rightarrow K^-p$  cross section, which however does not practically modify the  $p$ -wave amplitudes.

The results which we obtain for the  $p$ -wave amplitudes in this approach are consistent with experimental data for the differential cross sections. The contribution to the total cross sections at low energies is very small but in the differential cross sections its effects are clearly visible producing a slope in  $d\sigma/d\Omega$  as a function of  $\cos\theta$  which is in good agreement with the data.

One of the most interesting features of the  $p$ -wave in the  $S = -1$  sector is the presence of the  $\Sigma^*(1385)$  resonance below the  $K^-p$  threshold. This resonance cannot be generated dynamically from the strength of the  $p$ -wave in lowest order of the chiral Lagrangians and hence is introduced as a basic field, like the  $\Lambda$  or the  $\Sigma$ . It couples to the meson-baryon states with a strength obtained using SU(6) symmetry from the standard chiral Lagrangians involving pseudoscalar mesons and the octet of stable baryons. With these couplings and the unitarization procedure the  $\Sigma^*(1385)$  develops a width. In this sense, the total width of the  $\Sigma^*$ , as well as the branching ratios to  $\pi\Lambda$  and  $\pi\Sigma$ , are predictions of the theory and they come out with values in agreement with experiment.

The approach followed here corroborates once more the potential of the chiral Lagrangians to describe the low energy interaction of mesons with baryons, provided a fair unitarization procedure is used to appropriately account for the multiple scattering of the many channels which couple to certain quantum numbers. In this particular case, the previous works in the  $S = -1$  sector in  $s$ -wave, together with the present one for  $p$ -wave, provide a good theoretical framework to study the meson-baryon dynamics at low energies. These works show that the basic dynamical information is contained in the chiral Lagrangian of lowest order, since by means of a proper unitarization procedure in coupled channels and one regularizing parameter of natural size for the loops, one can describe quite well the low energy scattering data in the different reactions with  $S = -1$ .



## Acknowledgments

E. O. and D. J. wish to acknowledge the hospitality of the University of Barcelona. This work is also partly supported by DGICYT contract numbers BFM2000-1326, PB98-1247, by the EU TMR network Eurodaphne, contract no. ERBFMRX-CT98-0169, and by the Generalitat de Catalunya project 2001SGR00064.

## References

- [1] J. Gasser, H. Leutwyler, Nucl. Phys. B250 (1985) 465
- [2] U. G. Meissner, Rep. Prog. Phys. 56 (1993) 903
- [3] V. Bernard, N. Kaiser and U. G. Meissner, Int. J. Mod. Phys. E4 (1995) 193
- [4] A. Pich, Rep. Prog. Phys. 58 (1995) 563
- [5] G. Ecker, Prog. Part. Nucl. Phys. 35 (1995) 1
- [6] N. Kaiser, P. B. Siegel and W. Weise, Phys. Lett. B362 (1995) 23
- [7] N. Kaiser, P. B. Siegel and W. Weise, Nucl. Phys. A594 (1995) 325
- [8] N. Kaiser, T. Waas and W. Weise, Nucl. Phys. A612 (1997) 297
- [9] E. Oset and A. Ramos, Nucl. Phys. A635 (1998) 99
- [10] J. A. Oller and U. G. Meissner, Nucl. Phys. A673 (2000) 311
- [11] A. Gómez Nicola, J. Nieves, J.R. Peláez and E. Ruiz Arriola, Phys. Lett. B486 (2000) 77
- [12] J. Nieves and E. Ruiz Arriola, Phys. Rev. D64 (2001) 116008
- [13] J. C. Nacher, A. Parreño, E. Oset, A. Ramos, A. Hosaka and M. Oka, Nucl. Phys. A678 (2000) 187
- [14] T. Inoue, E. Oset and M. J. Vicente Vacas, Phys. Rev. C65 (2002) 035204
- [15] J. Caro Ramon, N. Kaiser, S. Wetzell and W. Weise, Nucl. Phys. A672 (2000) 249
- [16] J. A. Oller and U. G. Meissner, Phys. Lett. B500 (2001) 263
- [17] M. F. Lutz and E. E. Kolomeitsev, Nucl. Phys. A700 (2002) 193

- [18] E. Oset, A. Ramos and C. Bennhold, Phys. Lett. B527 (2002) 99
- [19] A. Ramos, E. Oset and C. Bennhold, nucl-th/0204044
- [20] E. Oset and A. Ramos, Nucl. Phys. A679 (2001) 616
- [21] D. Cabrera, E. Oset and M. J. Vicente Vacas, Nucl. Phys. A705 (2002) 90
- [22] J. A. Oller, E. Oset, Phys. Rev. D60 (1999) 074023
- [23] J. Ciborowski *et al.*, J. Phys. G8 (1982) 13
- [24] R. O. Bangerter, M. Alston-Garnjost, A. Barbaro-Galtieri, T. S. Mast, F. T. Solmitz and R. D. Tripp, Phys. Rev. D23 (1981) 1484
- [25] T. S. Mast, M. Alston-Garnjost, R. O. Bangerter, A. S. Barbaro-Galtieri, F. T. Solmitz and R. D. Tripp, Phys. Rev. D14 (1976) 13
- [26] M. Sakitt, T. B. Day, R. G. Glasser, N. Seeman, J. H. Friedman, W. E. Humphrey and R. R. Ross, Phys. Rev. 139 (1965) B719
- [27] T. S. Mast, M. Alston-Garnjost, R. O. Bangerter, A. S. Barbaro-Galtieri, F. T. Solmitz and R. D. Tripp, Phys. Rev. D11 (1975) 3078
- [28] P. Nordin, Jr, Phys. Rev. 123 (1961) 2168
- [29] D. Berley *et al.*, Phys. Rev. D1 (1970) 1996
- [30] M. Ferro-Luzzi, R. D. Tripp, and M. B. Watson, Phys. Rev. Lett. 8 (1962) 28
- [31] M. B. Watson, M. Ferro-Luzzi, and R. D. Tripp, Phys. Rev. 131 (1963) 2248
- [32] P. Eberhard *et al.* Phys. Rev. Lett. 2 (1959) 312
- [33] J.K. Kim, Phys. Rev. Lett. 21 (1965) 719
- [34] F. Barreiro *et al.* Nucl. Phys. B126 (1977) 319
- [35] D. E. Groom *et al.* [Particle Data Group Collaboration], Eur. Phys. J. C15 (2000) 1